Journal of Alloys and Compounds 834 (2020) 155132

Contents lists available at ScienceDirect

Journal of Alloys and Compounds

journal homepage: http://www.elsevier.com/locate/jalcom

Thermal stability and microhardness of metastable ω-phase in the Ti-3.3 at.% Co alloy subjected to high pressure torsion

Anna Korneva [a, *], Boris Straumal [b, c, d, e], Askar Kilmametov [b, d], Łukasz Gondek [f], Anna Wierzbicka-Miernik [a], Lidia Lityńska-Dobrzyńska [a], Grzegosz Cios [g], Robert Chulist [a], Paweł Zięba [a]

[a] Institute of Metallurgy and Materials Science, Polish Academy of Sciences, 25 Reymonta Street, 30-059, Kraków, Poland
[b] Karlsruhe Institute of Technology (KIT), Institute of Nanotechnology, 76344, Eggenstein-Leopoldshafen, Germany
[d] Scientific Center in Chernogolovka, Russian Academy of Sciences, Lesnaya Str. 9, Chernogolovka, 142432, Russia
[c] Institute of Solid State Physics, Russian Academy of Sciences, Ac. Ossipyan Str. 2, Chernogolovka, 142432, Russia
[e] National University of Science and Technology «MISIS», Moscow, 119049, Russia
[f] AGH University of Science and Technology, Faculty of Physics and Applied Computer Science, Mickiewicza 30 Avenue, 30-059, Kraków, Poland
[g] AGH University of Science and Technology, Academic Centre of Materials and Nanotechnology, Mickiewicza 30, 30-059, Kraków, Poland

ARTICLE INFO

Article history:
Received 28 August 2019
Received in revised form
8 April 2020
Accepted 9 April 2020
Available online 10 April 2020

Keywords:
Ti-based alloy
High pressure torsion
Phase transformations
Differential scanning calorimeter
High temperature X-ray diffraction
Transmission electron microscopy

ABSTRACT

The Ti−3.3 at.% Co alloy was annealed at 800 °C and then deformed by high-pressure torsion (HPT) at room temperature. The initial microstructure contains coarse grains of the α-phase uniformly distributed in the fine-lamellar (α+β) matrix. The study of the alloy after HPT by means of X-ray diffraction (XRD), scanning and transmission electron microscopy techniques showed strong grain refinement of the microstructure and the appearance of the high-pressure ω-Ti phase as the result of β→ω and partial α→ω phase transformations. It was found that the α→ω phase transformation depends not only on phase composition, but also on the shape and grains size as well (only fine lamellae of the α-Ti transformed into the ω-Ti phase). The formation of the ω-Ti phase doubled the hardness of the alloy. The thermal stability of the metastable ω-Ti phase, investigated by means of calorimetric and in-situ XRD measurements, increased from 180 °C to 375 °C in comparison to pure titanium.

© 2020 Elsevier B.V. All rights reserved.

1. Introduction

It is well known that severe plastic deformation (SPD) always induces strong grain refinement of microstructure. The possibility of modification of the microstructure, and consequently of the properties of materials, is therefore a widely understood aspect of SPD. Another aspect, to which less attention has been paid, is the phenomenon of SPD-driven phase transformations such as the formation [1] or decomposition of a supersaturated solid solution [2], dissolution of phases [3], amorphisation of crystalline phases [4], decomposition of an amorphous phase with the formation of nanocrystals [5], or allotropic phase transformations [6]. These phase transformations generally proceed due to the increased density of crystal lattice defects and the activation of diffusion processes, caused by the SPD.

Phase transformations, driven by SPD, are especially effective for titanium since it possesses three allotropic variations: the low-temperature α-Ti with a hexagonal close-packed crystal structure (space group P63/mmc), the high-temperature β-Ti with body-centered cubic structure (space group Im3m), and the high-pressure ω-Ti with a hexagonal structure (space group P6/mmm). It was found that, in the Ti-based alloys, the ω-Ti phase forms more easily from the β-Ti phase during SPD [7], and also from the α-Ti phase under pressure between 2 and 8 GPa, depending on the experimental technique, pressure environment and alloying additions [8]. It should be noted that the α→ω and β→ω phase transformations are martensitic (diffusionless). The formation of the ω-phase in Ti is related to the specific electronic structure, which is characterised by the relationship between the occupied narrow *d* bands and the broad *sp* bands. Under the applied pressure, the *sp* bands rise faster in energy, causing electrons to be transferred to the *d* bands [9]. This process is known as the *s-d* transition, and it

* Corresponding author.
E-mail address: a.korniewa@imim.pl (A. Korneva).

https://doi.org/10.1016/j.jallcom.2020.155132
0925-8388/© 2020 Elsevier B.V. All rights reserved.

governs the structural properties of the transition metals. It was found that external shear stress and the alloying of pure Ti with β-stabilising elements such as the *d*-electron rich transition elements (for example, Co, V, Mo, Fe, Ni or Nb), provide an additional driving force for the α→ω or β→ω transformations [10].

The formation of the ω-phase at high pressures raises a number of scientific and engineering issues, mainly because the ω phase is fairly brittle compared with the α-phase, which may significantly limit the use of Ti in high-pressure conditions [11]. On the other hand, it was found that a short annealing of pure Ti, previously deformed by HPT resulted in improved strength and ductility [12] and a reversal of the ω→α transformation [13]. Therefore, it was assumed that this reverse transformation improves the mechanical properties of the Ti-based alloys. In this work, the Ti—Co system was chosen for the study of the fundamentals of α↔ω phase transformation. Ti—Co based alloys are broadly used in many branches of industry, especially in dentistry and medicine [14], because alloying with Co improves the corrosion resistance [15] and mechanical properties [16] of Ti, and reduces its melting temperature of Ti, which can resolve many casting problems. However, detailed knowledge of the fundamentals of the ω-phase formation at high pressure, and of its thermal stability at elevated temperatures, is still lacking for the Ti—Co based alloys. In our previous work [17], the formation of the ω-phase under HPT condition was studied for the Ti—3.3 at.%Co (or Ti-4wt.% Co) alloy contained the α-phase and Ti_2Co intermetallic phase. The (α+Ti_2Co) state of microstructure was obtained using anneals below the temperature of eutectoid transformation. In the current work the Ti—3.3 at.%Co alloy was annealed above the temperature of eutectoid transformation in order to obtain the (α+β) phase composition. The main aims of this work were the study of the fundamentals of the (α+β)↔ω phase transformation in Ti—3.3 at.%Co alloy, caused by HPT, as well as the study of the ω-phase thermal stability and the influence of the ω-phase on the microhardness of the examined alloy.

2. Material and methods

Pure titanium (99.98%) and cobalt (99.99%) were used for preparation of the Ti—3.3 at.% Co alloy. The alloy was melted in an induction furnace in a pure argon atmosphere. The obtained cylindrical ingots of the alloy with a diameter of 10 mm were cut by spark erosion into discs with a thickness of 0.7 mm. The samples were then sealed in quartz ampoules and annealed at a temperature of 800 °C for 720 h in a vacuum at a residual pressure of 4×10^{-4} Pa. After annealing, the samples, still inside the ampoules, were quenched in water. The annealed samples were subjected to HPT at room temperature under pressure of 7 GPa for five full rotations, at a deformation rate of 1 rpm, in a Bridgman anvil type unit using a custom-built computer-controlled device manufactured by W. Klement GmbH, Lang, Austria. X-ray diffraction (XRD) was carried out using a Siemens D-500 X-ray diffractometer with Cu-*Kα* radiation. Phase analysis and calculation of lattice parameters were performed with the help of PowderCell for Windows Version 2.4.March 08, 2000 (Werner Kraus & Gert Nolze, BAM Berlin). The microstructure observations were carried out using an FEI E-SEM XL30 scanning electron microscope equipped with an EDAX Genesis energy-dispersive X-ray spectrometer (EDS). The SEM images were taken using backscattered electron signal (BSE) mode, in order to obtain the composition contrast between different phases. Transmission electron microscopy (TEM) investigations were carried out using a TECNAI G2 FEG super TWIN (200 kV) with EDS manufactured by EDAX. The thin foils for TEM observation of initial microstructure were prepared using a twin-jet polishing technique with a D2 electrolyte manufactured by Struers. The focused ion beam (FIB) technique was applied by means of FIB Quanta 3 D, TECNAI FEG microscopy (30 kV) for the preparation of thin foils of deformed materials, in order to obtain the interface between the α-Ti phase and the (α+β) matrix. The in-situ XRD studies were carried out using a Panalytical Empyrean diffractometer (Cu-*Kα* radiation) equipped with an Anton Paar HTK 1200 high-temperature chamber. The bulk samples were placed on an Al_2O_3 sample holder and introduced into the chamber, which was consequently evacuated, then flushed and filled with high purity (6 N) Ar gas. During measurements, the thermal displacement of the sample was cancelled by the appropriate movement of the chamber. Samples were heated at a rate of 5 °C/min, and diffraction patterns were collected in steps of 20 °C up to 800 °C. The 2θ range was chosen between 30 °C and 80 °C with a step size of 0.01667°. The acquisition time per single pattern was 80 min. A differential scanning calorimeter (DSC 404 F1 Pegasus, Netzsch) was used for the calorimetric measurements. The samples were heated up to 800 °C in an argon atmosphere, in the Al_2O_3 crucibles at the rate of 20 °C/min. The hardness was measured using an AGILENT G200 nanoindenter with XP head at a load of 96 mN. The hardness of individual phases was measured (before and after deformation) at a distance of half the radius of the sample discs. Each hardness value is an average of 10 measurements.

3. Results and discussion

The microstructure of the Ti-3.3 at.% Co alloy after annealing at 800 °C contains the coarse grains of the α-phase (sizes of about 200 μm), uniformly distributed in the fine-lamellar (α+β) matrix (Fig. 1). The structure of both phases of the matrix was identified by selected area electron diffraction (SAED) patterns presented in Fig. 1e and f. The volume fraction of the coarse α-phase grains was about 16%. According to the Ti—Co phase diagram, the solubility of Co in the α-Ti and β-Ti solid solutions is different, reaching 1.2 at.% and 14.5 at.%, respectively [18]. Measurement of the chemical composition by means of EDS in TEM showed that only the coarse α-Ti phase grains contain about 0.7 ± 0.2 at.%Co, while the fine-lamellar α-phase grains do not contain cobalt. The β-phase contains up to 12 at.% Co. Analysis of XRD patterns (Fig. 2) also confirms the presence of peaks only from the α-Ti and β-Ti phases, with the volume fraction of about 70% and 30%, respectively (Table 1). A detailed examination of the diffractogram (see the upper right corner of Fig. 2) showed a splitting of the main α-Ti phase peak (00.2) into two sub-peaks. This means that grains of the α-Ti phase have two different plane spacings corresponding to a change of parameter *c* of the lattice cell. The first sub-peak corresponds to 2.353 Å of plane spacing and $c = 0.4706$ nm, and the second one to 2.343 Å and $c = 0.4688$. Since cobalt reduces the lattice parameters of titanium, it was assumed that the second sub-peak corresponds to the coarse α-Ti phase grains, and the first one to the lamellar α-Ti phase. It should be noted, that the 00.2 plane of the α-Ti phase is the basal plane of the α→ω transformation.

Fig. 3 presents the microstructure of the alloy after HPT. The coarse grains of the α-Ti phase, elongated in the direction of shear deformation, are visible. TEM observation of deformed material showed a high dislocation density inside the coarse α-phase grains. They did not undergo any fragmentation or refinement (Fig. 3b and c) and only two or three low-angle grain boundaries were observed within the α grains), while the fine-lamellar matrix was strongly refined (Fig. 3d and e). The size of grains, observed in the dark field image (Fig. 3e), varied between 50 and 100 nm. Analysis of SAED patterns (one SAED is presented as an example in (Fig. 3f) showed that only one or two rings belong to the α-phase, and the remaining eight or nine belong to the ω-Ti phase. Analysis of the XRD pattern of the deformed alloy also confirmed that most of the peaks belong

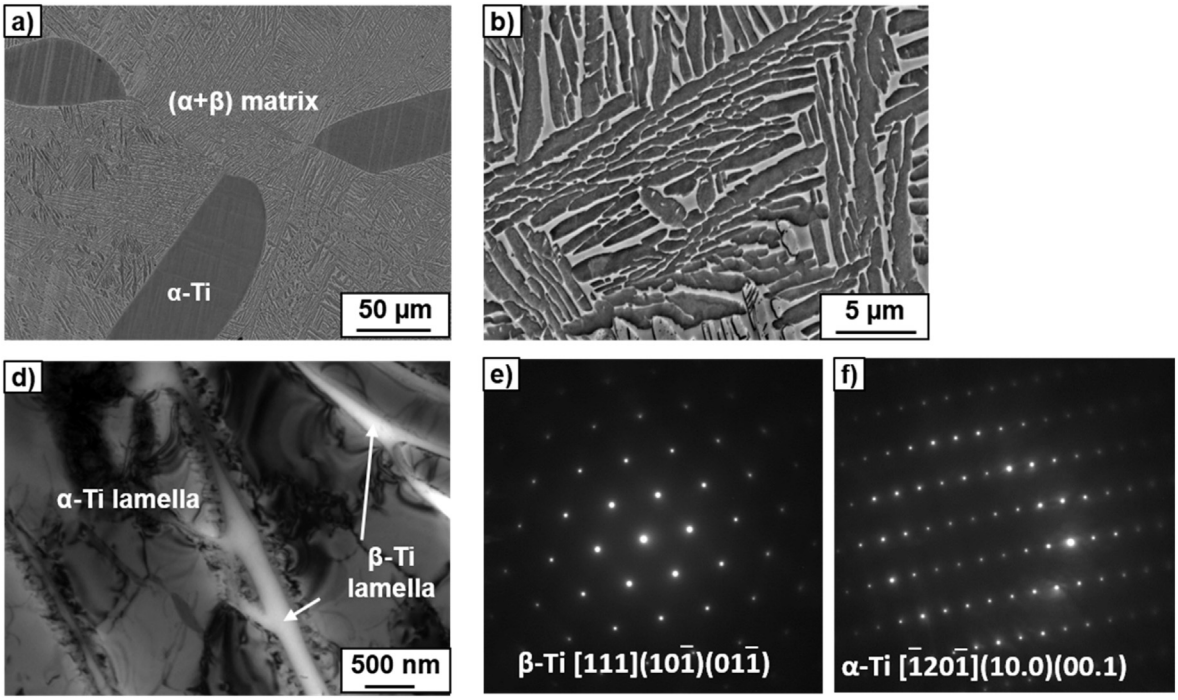

Fig. 1. SEM/BSE microstructures (a, b) and TEM-bright field image (d) of the Ti–3.3 at.% Co alloy after annealing at 800 °C. The β-Ti phase reveals a bright contrast in the SEM/BSE images. SAED patterns of the α- and β-phase lamellae are presented in (e) and (f), respectively.

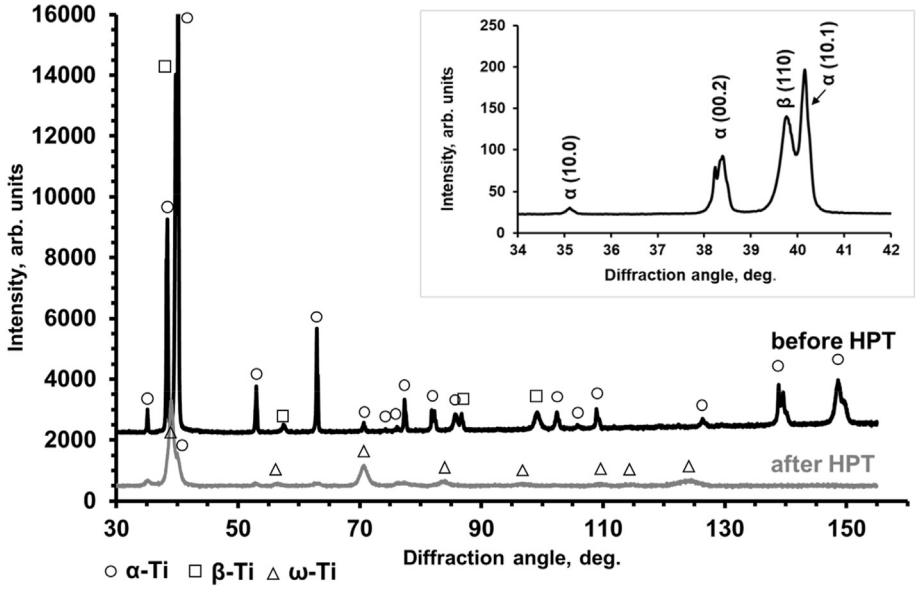

Fig. 2. X-ray diffraction patterns of the Ti–3.3 at.%Co alloy before and after HPT. An enlarged part of the diffractogram of the alloy before HPT is presented in the upper right corner of the figure.

Table 1
Lattice parameters and volume fraction of different phases observed in the Ti-3.3 at.%Co alloy before and after HPT.

Phase	Lattice parameters, nm		Volume fraction, %	
	Before HPT	After HPT	Before HPT	After HPT
α-Ti	$a = 0.2950 \pm 0.0001$ $c = 0.4697 \pm 0.0001$	$a = 0.2952 \pm 0.0001$ $c = 0.4708 \pm 0.0001$	70	17
β-Ti	0.3204 ± 0.0001	–	30	0
ω-Ti	–	$a = 0.4617 \pm 0.0001$ $c = 0.2826 \pm 0.0001$	0	83

to the ω-phase, with a volume fraction of about 83% (Table 1), that the peaks from the α-Ti phase became smaller, and that some peaks from the α-phase and all peaks from the β-phase disappeared. All observed peaks are significantly broadened, suggesting a strong grain refinement and significant micro-distortion of the crystal lattices. Therefore, it can be concluded that HPT resulted in the partial α→ω and full β→ω phase transformations. Since the amount of the α-phase after HPT (17%) is almost equal to the amount of the coarse grains of the α-Ti phase before HPT (16%), it can be established that the latter did not transform into the ω-Ti

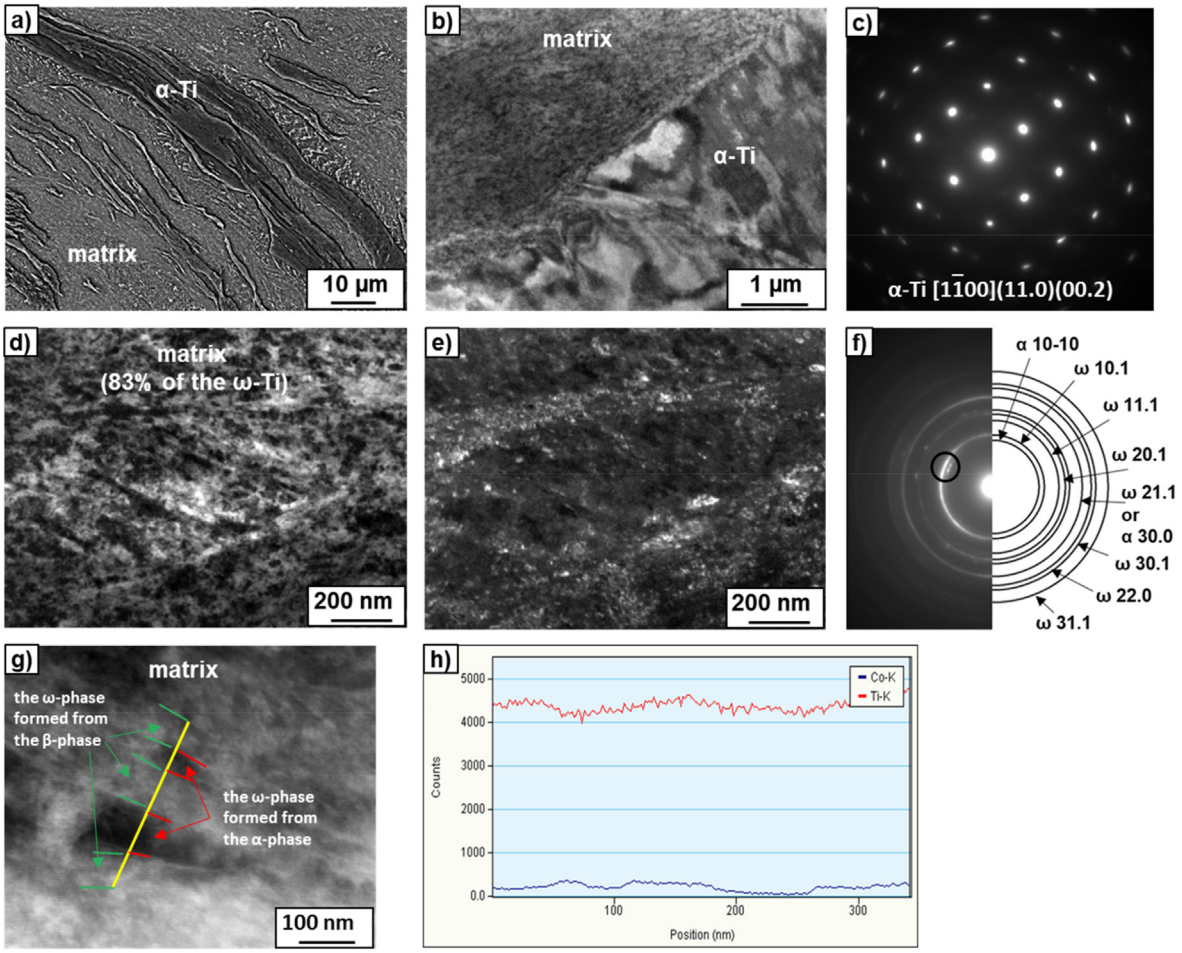

Fig. 3. SEM (a), TEM (b–f) and STEM (g) images of microstructure of the Ti–3.3 at.% Co alloy after HPT. TEM-bright field image (b) presents the interface between matrix and coarse grain of the α-phase. SAED patterns (c) from the α-phase observed in the (b) image. Bright field (d), dark field (c) TEM images and SAED pattern (f) from the deformed matrix. (h) Distribution of Co and Ti content along the line, marked in (g).

phase during HPT. It is possible that increased density of dislocations in the coarse α-Ti grains alone (without any fragmentation) is insufficient for the start of the α→ω transformation. D. Trinkle [19] showed that, for the α→ω transformation, a certain energy barrier has to be overcame, which can be associated with the accumulation of stresses in microstructure. It is possible that a fine two-phase (α+β) plate-like matrix is more easily deformed than large grains of the α-Ti phase. Therefore, the fine grains of the α-Ti phase overcome the critical shear stresses necessary for this transformation. It is possible also that coarse α-Ti grains have an unfavorable grains orientation for the activation of slip systems responsible for the α→ω-phase transition.

At the same time, the formation of the ω-phase during HPT depends on an initial state of the microstructure. In particular, the α→ω transition depends on the phase composition (i.e. α, β-phases, intermetallic compounds) and the microstructure features of different phases (grain size, shape). For example, the formation of ω-Ti phase from the (α+Ti_2Co) state was studied early [17]. It was found that the volume fraction of the ω-Ti phase depends on the content of the alloying element in the grains of the α-phase.

It should be noted that the lattice parameters of the α-phase after HPT increased insignificantly, indicating a decrease of Co content [20]. This behaviour is very similar to the "purification" of the α-Ti phase and the α′-Ti martensite after HPT observed in the binary Ti–Fe alloys [21]. It is possible that Co atoms during HPT migrated from the α-phase into the newly-formed ω-Ti phase. A similar situation was observed in the Ti–Fe alloy subjected to HPT, in which it was found that the solubility of Fe in ω-Ti is much higher than in the α-Ti phase [7]. The measurements of Co content along the line in the deformed matrix of the Ti–3.3 at.%Co alloy (Fig. 3g and h) showed that the grains of the ω-Ti phase formed from the α-Ti and β-Ti grains contain different amount of Co. The Co concentration in the ω-Ti phase formed from the α-Ti and from β-Ti phases reached about 0.2–0.5 and 4.0–6.2 at.%, respectively. These data have a good agreement with the work [7], where the content of the alloying element in the ω-phase appeared revealed to be dependent on the initial phase before transformation.

The microhardness measurements showed that the hardness of the coarse α-Ti phase grains and fine-lamellar (α+β) matrix reached 5.2 GPa and 3.4 GPa before HPT. It is possible that the β-Ti phase with the bcc structure greatly reduces the hardness of the matrix. After HPT, the hardness of the coarse α-Ti phase increased to only 6.0 GPa, while the hardness of the matrix (containing about 83% of the new-formed ω-Ti phase) increased significantly to 6.7 GPa. It is possible that, at the first stages of HPT, only the matrix was deformed, and when its hardness reaches the hardness of the coarse α-Ti phase grains, the latter began to deform too. A slight increase in the hardness of the coarse α-Ti phase grains confirms the accumulation of a small degree of deformation.

Results of the study of thermal stability of the metastable ω-Ti phase by means of DSC and in-situ XRD measurements are presented in Fig. 4. One small endothermic peak is observed on the heating DSC curve of the annealed sample, whereas two exothermic peaks and one endothermic peak are detected for the deformed alloy (Fig. 4a). According to the Ti–Co equilibrium phase diagram, the eutectoid transformation $\beta \rightarrow (\alpha + Ti_2Co)$ takes place at a temperature of 685 °C. Therefore, the endothermic peaks observed in the temperature range of 689 °C–726 °C (annealed sample) and 699 °C–725 °C (deformed sample) are associated with the dissolution of the Ti_2Co phase. However, this intermetallic phase was not observed in the annealed state or in the deformed sample. Thus, it was assumed that the Ti_2Co phase appeared under heating of the samples in the calorimeter. Consequently, the exothermic peak observed in the temperature range of 457 °C–500 °C for the deformed sample, is related with the precipitation of the Ti_2Co particles. In order to confirm this statement, the thin foil of the deformed sample was subjected to isothermal annealing in the DSC equipment, at up to 500 °C for 10 min, and then studied using TEM. Analysis of electron diffraction patterns and the measurement of chemical composition of the prepared sample confirmed the presence only of the Ti_2Co particles, uniformly distributed in the α-Ti matrix (Fig. 5). Next, it was assumed that the exothermic peak, observed at the lower temperatures between 400 °C and 445 °C (Fig. 4b) can be related with the reverse transformation of the ω-Ti phase into the α-Ti one. It should be noted that the process of dissolution of stable phases is endothermic, whereas the decomposition of metastable phases occurs with the release of heat (an exothermic reaction), because these types of phases are characterised by an excess of energy. The author's previous DSC study of this alloy after HPT (but annealed in a temperature range of 400 °C–600°C) also showed that the reverse process of $\omega \rightarrow \alpha$ transformation occurred in a similar temperature range of 370 °C–444°C. The question is, if the deformed material contains 83% of the ω-Ti phase, why is the peak on the DSC heating curve responsible for the reverse transformation of this phase so small as to be almost invisible? The in-situ XRD study provides the answer to this question (Fig. 4c). Only one main peak (11.0) of the ω-Ti phase (Fig. 4c) is observed in the deformed alloy before heating at the diffraction angles range of 34°–42°. The intensity of this peak remained almost the same under heating up to 275 °C. Then, its intensity increased significantly at heating up to 375 °C, and simultaneously the weak reflections (00.2) and (10.1) of the α-Ti phase appeared. The appearance of these α reflections (from the left and right side of the (11.0) ω-peak, Fig. 4 c) indicates the beginning of the $\omega \rightarrow \alpha$ transition, while the significant increase in intensity of the (11.0) ω reflection is related to the appearance of athermal ω-phase. The athermal ω-phase generally forms during quenching from the β region, or during aging at temperatures between 300 °C and 400 °C for the Ti–Co based alloys with 3.3 at.% to 10 at.% Co [18]. Thus, two opposed processes are observed simultaneously in the temperature range of 275 °C–375 °C: the start of transition of the deformation-induced ω-phase to the α-Ti phase, and the appearance of the athermal ω-phase. This explains why the peak in the temperature range of 400 °C–445 °C on the DSC curve is so small as to be almost invisible. Further in-situ XRD heating above 375 °C resulted in the complete disappearance of the (11.0) ω-Ti peak and the appearance of additional peaks from the α-Ti phase (10.0) and Ti_2Co particles (422) and (511). This means that the ω-Ti phase decomposed into the α-Ti phase and Ti_2Co particles. It should be noted that the splitting and subsequent significant displacement of α-Ti (10.0) and (10.1) peaks towards the lower diffraction angles are observed at a heating temperature of almost 550 °C. This indicates that the α-Ti phase formed after decomposition of the ω-Ti phase is enriched in Co, and that heating above 550 °C resulted in its disappearance and the formation a new α-Ti cells free of the cobalt atoms. In other words, the new α-Ti phase is more in equilibrium and its lattice parameters ($a = 0.2959$ nm, $c = 0.4710$ nm) are close to pure titanium ($a = 0.2955$ nm, $c = 0.4694$ nm). It is possible that Co atoms segregate at grain boundaries, the volume fraction of which increased significantly due to the strong grain refinement of the deformed material [11]. The process of $\alpha + Ti_2Co \rightarrow \beta$ transformation and the formation of Ti_2O are also observed at higher temperatures of heating (about 700 °C).

Summarising the results obtained from DSC and in-situ XRD measurements, it can be stated that the ω-Ti phase decomposed under heating above 445°C according to the DSC study (at a heating rate of 20 °C/min) and above 375°C according to the in-situ XRD measurement (at a heating rate of 5 °C/min). The shift of the temperature range of the $\omega \rightarrow \alpha$ reverse phase transformation,

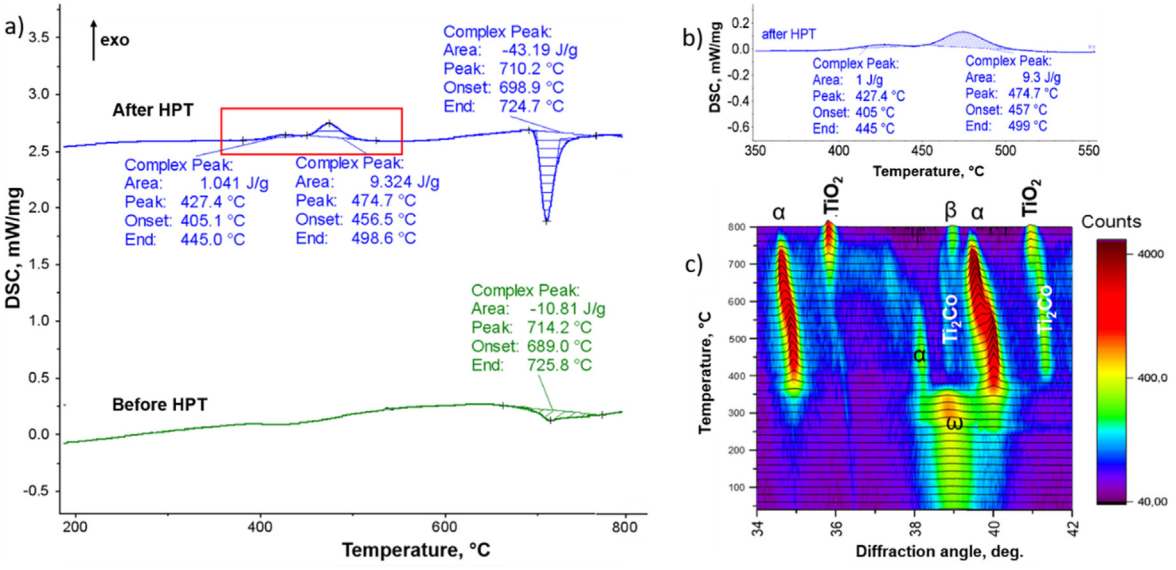

Fig. 4. DSC heating curves of the Ti–3.3 at.% Co alloy before and after HPT (a). The part of the heating curve marked by the red rectangle in (a) is presented in enlarged scale in (b). In-situ XRD map (c) of the deformed alloy. (For interpretation of the references to colour in this figure legend, the reader is referred to the Web version of this article.)

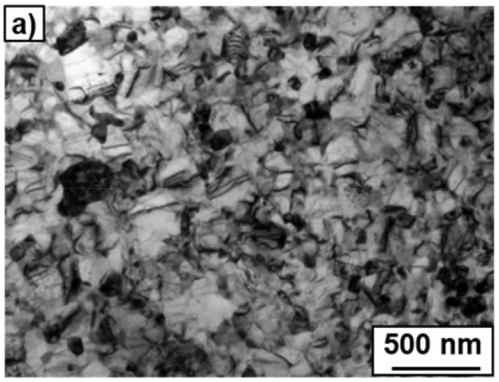

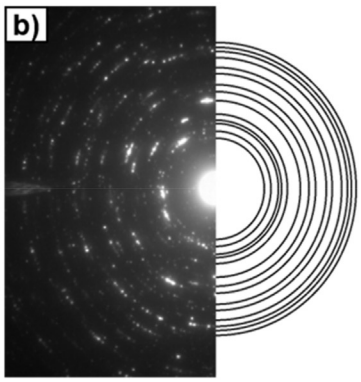

d [Å]	Phase	hkl
2.566	Ti	10.0
2.260	Ti	10.1
1.989	Ti_2Co	440
1.885	Ti_2Co	442
1.732	Ti	10.2
1.468	Ti_2Co	731
1.335	Ti_2Co	660
1.245	Ti_2Co	842
1.124	Ti_2Co	771
1.067	Ti	10.4
0.988	Ti	20.3
0.942	Ti	21.1
0.918	Ti	11.4
0.886	Ti	10.5

Fig. 5. TEM bright field image (a) and SAED pattern (b) of the Ti–3.3 at.% Co alloy after HPT and heating in the calorimeter at 500 °C for 10 min. Table with data of phases and Miller indices (hkl) corresponding to the rings on the SAED pattern is also presented in (b).

depending on the heating rate, may indicate the diffusion nature of this transformation, or the contribution of a diffusion process to the transformation. It should be noted that the mechanism of this transformation has not yet been fully studied in the literature. T. Low and S. Niezgoda [22] claimed that the ω→α transformation is being hindered by defects in the ω-phase. They found a significant reduction of dislocation densities in the ω-phase prior to initiation of the reverse ω→α transformation. Since the annihilation of dislocation is a thermally-activated process, the higher the heating rate is, the higher are the temperatures for the occurrence of reverse transformation.

It should be noted that, in the pure Ti, the volume fraction of the ω phase induced by HPT (under the same conditions) reached only 40% [7], and the process of reverse ω→α transformation is finished at 180 °C under heating at a rate of 10 °C/min [13]. Therefore, the alloying of pure Ti with 3.3 at.% of Co results in the significant increase of volume fraction of the ω-Ti phase and its thermal stability.

One can also compare the obtained results with in-situ XRD of Ti–Fe alloys annealed in the α plus β area of the Ti–Fe phase diagram and subjected to HPT [23]. In the case of Ti–Fe alloys, the thermal stability of ω-Ti phase is higher, disappearing under heating at around 500 °C.

4. Conclusions

HPT resulted in strong grain refinement of the fine-lamellar (α+β)-matrix and its transformation into the metastable ω-Ti phase with different amounts of cobalt depending on the distribution of the former α and β lamellae.

The formation of the ω-phase depends on the state of the initial microstructure, i.e. from phase composition and microstructure features of various phases. In particular, fine lamellae of the α-Ti phase transform into the ω-Ti phase, while the coarse α-Ti phase grains contain only the high dislocation density and do not exhibit phase transformation.

HPT led to a slight increase of the hardness of the coarse α-Ti phase grains (from 5.2 GPa to 6.0 GPa), and to a two-fold increase of the hardness of the fine matrix (from 3.4 GPa to 6.7 GPa) due to the formation of the ω-Ti phase.

The temperature range of the reverse ω→α transformation depends on the heating rate of the deformed samples: the higher the heating rate, the greater the shift of the temperature range of the phase transformation towards higher temperatures. It is possible that the process of annihilation of dislocations in the ω-Ti phase is responsible for this behaviour.

The alloying of titanium with 3.3 at.% of cobalt results in the significant increase of the volume fraction of the ω-phase and its thermal stability from 180°C, to 375 °C to 445°C in comparison to pure titanium.

Declaration of competing interest

The authors declare that they have no known competing financial interests or personal relationships that could have appeared to influence the work reported in this paper.

CRediT authorship contribution statement

Anna Korneva: Visualization, Investigation, Validation, Resources, Data curation, Writing - original draft, Writing - review & editing, Funding acquisition. **Boris Straumal:** Conceptualization, Validation, Resources, Funding acquisition. **Askar Kilmametov:** Conceptualization, Validation, Investigation, Writing - review & editing. **Łukasz Gondek:** Investigation. **Anna Wierzbicka-Miernik:** Investigation. **Lidia Lityńska-Dobrzyńska:** Investigation. **Grzegosz Cios:** Investigation. **Robert Chulist:** Investigation. **Paweł Zięba:** Validation.

Acknowledgements

This work is supported by National Science Centre of Poland (grant OPUS 2017/27/B/ST8/0 1092), by Deutsche Forschungsgemeinschaft (project numbers IV 98/5-1, HA 1344/32-1) and Russian Foundation for Basic Research (grant 18-03-00067).

References

[1] V. Stolyarov, R. Lapovok, I. Brodova, P. Thomson, Ultrafine-grained Al–5 wt.% Fe alloy processed by ECAP with backpressure, Mater. Sci. Eng., A 357 (2003) 159–167, https://doi.org/10.1016/S0921-5093(03)00215-6.
[2] B. Straumal, A. Korneva, P. Zięba, Phase transitions in metallic alloys driven by the high pressure torsion, Arch. Civ. Mech. Eng. 14 (2014) 242–249, https://doi.org/10.1016/j.acme.2013.07.002.
[3] S. Ohsaki, S. Kato, N. Tsuji, T. Ohkubo, K. Hono, Bulk mechanical alloying of Cu–Ag and Cu/Zr two-phase microstructures by accumulative roll-bonding proces, Acta Mater. 55 (2007) 2885–2895, https://doi.org/10.1016/j.actamat.2006.12.027.
[4] A.V. Sergueeva, C. Song, R.Z. Valiev, A.K. Mukherjee, Structure and properties of amorphous and nanocrystalline NiTi prepared by severe plastic deformation and annealing, Mater. Sci. Eng., A 339 (2003) 159–165, https://doi.org/10.1016/S0921-5093(02)00122-3.
[5] A.M. Glezer, M.R. Plotnikova, A.V. Shalimova, S.V. Dobatkin, Severe plastic deformation of amorphous alloys: I. Structure and mechanical properties, Bull. Russ. Acad. Sci. Phys. 73 (2009) 1233–1239.
[6] X.L. Wang, L. Li, W. Mei, W.L. Wang, J. Sun, Dependence of stress-induced omega transition and mechanical twinning on phase stability in metastable β Ti–V alloys, Mater. Char. 107 (2015) 149–155, https://doi.org/10.1016/j.matchar.2015.06.038.
[7] A.R. Kilmametov, Yu Ivanisenko, A.A. Mazilkin, B.B. Straumal, et al., The α→ω

and β→ω phase transformations in Ti-Fe alloys under high-pressure torsion, Acta Mater. 144 (2018) 337–351, https://doi.org/10.1016/j.actamat.2017.10.051.
[8] A.K. Singh, M. Mohan, C. Divakar, Pressure-induced alpha-omega transformation in titanium: features of the kinetics data, J. Appl. Phys. 54 (1983) 5721–5730, https://doi.org/10.1063/1.331793.
[9] S.C. Gupta, K.D. Joshi, S. Banerjee, Experimental and theoretical investigations on d and f electron systems under high pressure, Metall. Mater. Trans. 39 (2008) 1593–1601, https://doi.org/10.1007/s11661-007-9377-1.
[10] J.R. Patel, M. Cohen, Criterion for the action of applied stress in the martensitic transformation, Acta Mettal 1 (1953) 531–538, https://doi.org/10.1016/0001-6160(53)90083-2.
[11] N. Velisavljevic, S. MacLeod, H. Cynn, Titanium alloys at extreme pressure conditions, in: N. Amin (Ed.), Titanium Alloys - Towards Achieving Enhanced Properties for Diversified Applications, InTech, 2012, pp. 67–86, https://doi.org/10.5772/36038.
[12] R.Z. Valiev, A.V. Sergueeva, A.K. Mukherjee, The effect of annealing on tensile deformation behavior of nanostructured SPD titanium, Scripta Mater. 49 (2003) 669–674, https://doi.org/10.1016/S1359-6462(03)00395-6.
[13] Y. Ivanisenko, A. Kilmametov, H. Rösner, R.Z. Valiev, Evidence of α→ω phase transition in titanium after high pressure torsion, Int. J. Math. Res. 99 (2008) 36–41, https://doi.org/10.3139/146.101606.
[14] K. Wang, The use of titanium for medical applications in the USA, Mater. Sci. Eng., A 213 (1996) 134–137, https://doi.org/10.1016/0921-5093(96)10243-4.
[15] J. Onagawa, Preparation of high corrosion resistant titanium alloys by spark plasma sintering, J. Jpn. Inst. Metals 63 (1999) 1149–1152, https://doi.org/10.2320/jinstmet1952.63.9_1149.
[16] Q. Liu, W.Y. Yang, G.L. Chen, On superplasticity of two phase alpha-titanium-intermetallic Ti–(Co, Ni)–Al alloy, Acta Metall. Mater. 43 (1995) 3571–3582, https://doi.org/10.1016/0956-7151(95)00032-Q.
[17] B. Straumal, A. Korneva, A.R. Kilmametov, L. Lityńska-Dobrzyńska, A.S. Gornakova, R. Chulist, M.I. Karpov, P. Zięba, Structural and mechanical properties of Ti–Co alloys treated by high pressure torsion, Materials 12 (2019) 426–437, https://doi.org/10.3390/ma12030426.
[18] J.L. Murray, The Co-Ti (Cobalt-Titanium) system, Bull. Alloy Phase Diagrams 3 (1) (1982) 74–85.
[19] D.R. Trinkle, D.M. Hatch, H.T. Stokes, R.G. Hennig, R.C. Albers, Systematic pathway generation and sorting in martensitic transformations: titanium α to ω, Phys. Rev. B 72 (2005), 014105 https://doi.org/10.1103/PhysRevB.72.014105.
[20] B.B. Straumal, A.R. Kilmametov, Yu Ivanisenko, A.A. Mazilkin, et al., Diffusive and displacive phase transitions in Ti–Fe and Ti–Co alloys under high pressure torsion, J. Alloys Compd. 735 (2018) 2281–2286, https://doi.org/10.1016/j.jallcom.2017.11.317.
[21] A. Kilmametov, Yu Ivanisenko, B. Straumal, A.A. Mazilkin, et al., Transformations of α' martensite in Ti–Fe alloys under high pressure torsion, Scripta Mater. 136 (2017) 46–49, https://doi.org/10.1016/j.scriptamat.2017.04.010.
[22] T.S.E. Low, S.R. Niezgoda, Modeling the α/ω thermal stability in shocked Zr: a coupling between dislocation removal and phase transformation, Acta Mater. 156 (2018) 104–115, https://doi.org/10.1016/j.actamat.2018.06.004.
[23] M.J. Kriegel, A. Kilmametov, M. Rudolph, B.B. Straumal, A.S. Gornakova, H. Stöcker, Y. Ivanisenko, O. Fabrichnaya, H. Hahn, D. Rafaja, Transformation pathway upon heating of Ti–Fe alloys deformed by high-pressure torsion, Adv. Eng. Mater. 20 (2018), 1700933, https://doi.org/10.1002/adem.201700933.